Electronic Supplementary Information

Improved Transparency in Highly Conductive Copper Chromium Oxide Coatings through Mg Doping and Stoichiometry Control

Jaewon Kim[a,b], Owen Kendall[b], Triet Thien Huu Nguyen,[b] Joel van Embden[b], Enrico Della Gaspera[b]

[a] *Institute of Materials Research and Engineering, Agency for Science, Technology and Research, 2 Fusionopolis Way, Singapore 138634, Singapore*

[b] *School of Science, RMIT University, Melbourne VIC 3000, Australia*

Correspondence should be addressed to: jaewon_kim@imre.a-star.edu.sg and enrico.dellagaspera@rmit.edu.au.

Figure S1. Compositional analysis via EDX of the $CuCrO_2$ films. Left panel: experimental vs. nominal Mg amount. Right panel: amount of Cu and (Cr+Mg) as a function of the amount of Mg introduced.

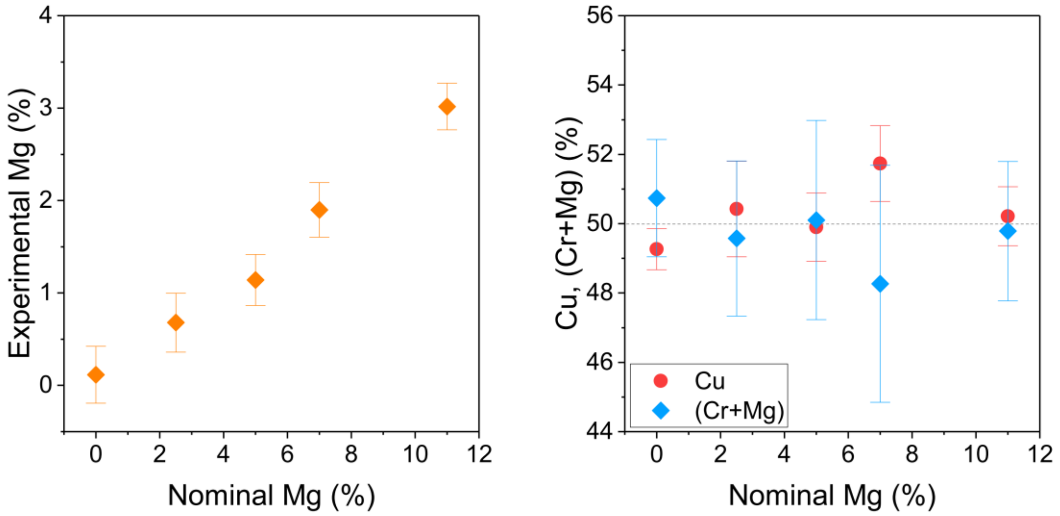

Figure S2. XRD patterns of Mg-doped $CuCrO_2$ coatings highlighting the main diffraction peak at ~36.5°. The black vertical dash line represents the expected (012) peak position according to ICDD No. 74-0983.

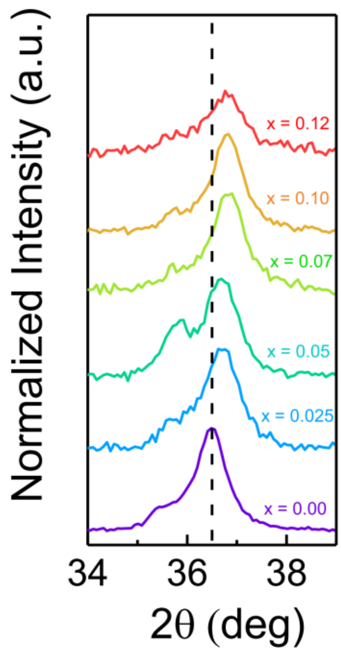

Figure S3. SEM top view images for the $CuCrO_2$ coatings at various Mg dopant concentrations from x= 0 (undoped) to x = 0.12. The scale bar is 2 μm for all the low-magnification images and 400 nm for all the high-magnification images.

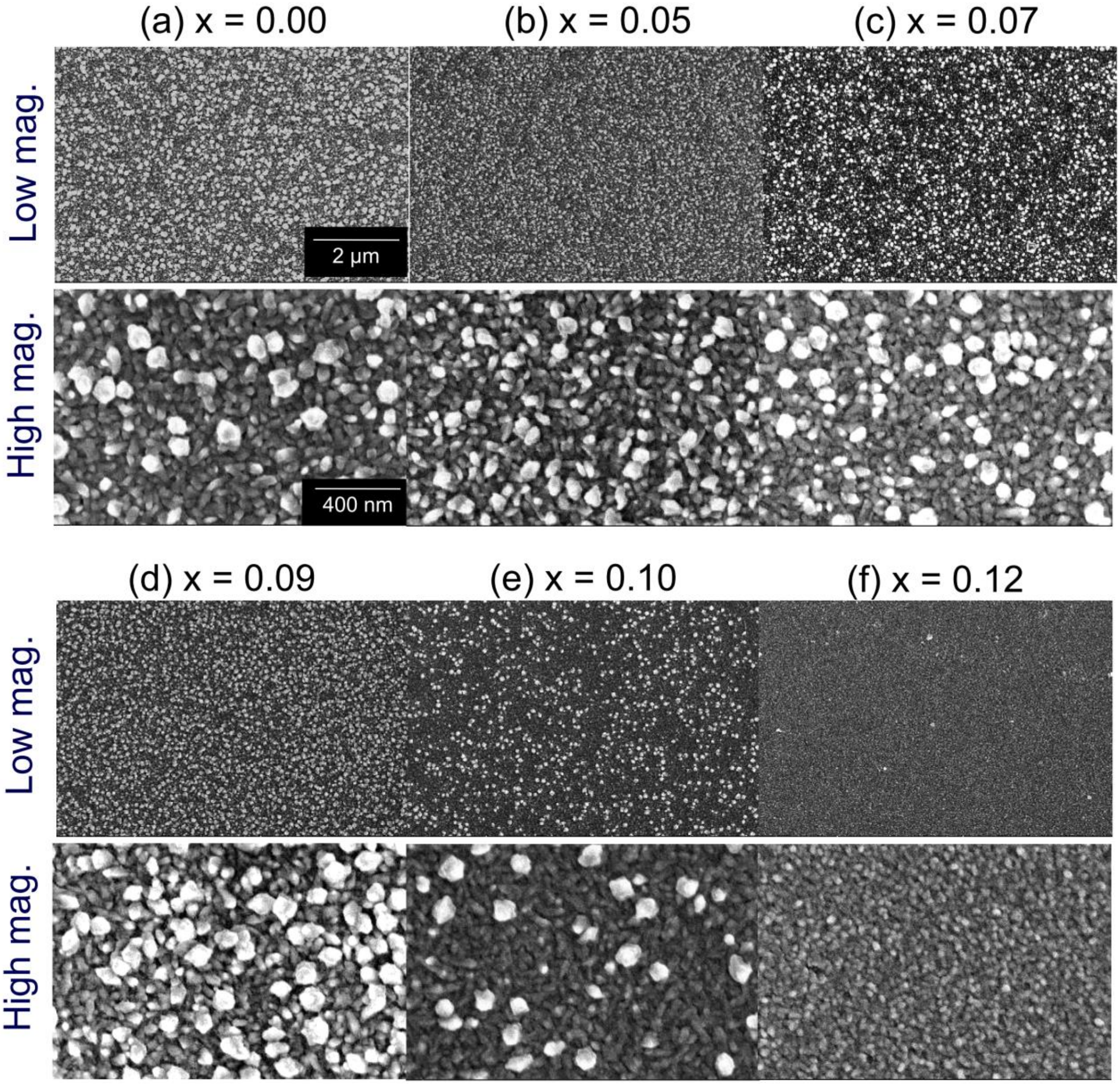

Figure S4. Cross-sectional SEM images for $CuCrO_2$ films at different Mg concentrations. The scale bar is 200 nm and is common to all panels.

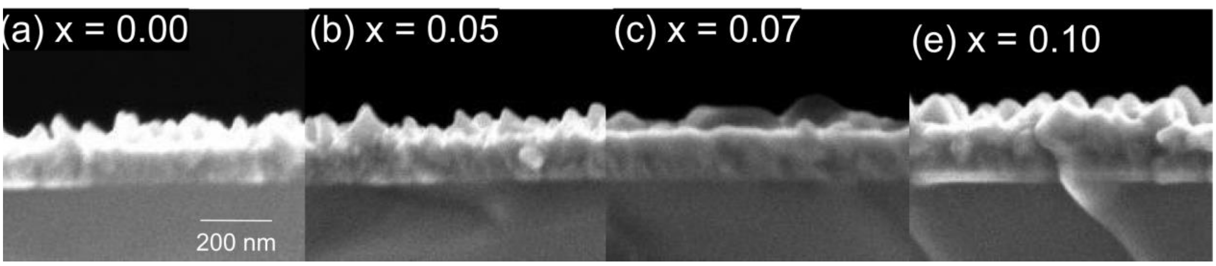

Figure S5. XPS survey spectrum of a typical Mg-doped $CuCrO_2$ film.

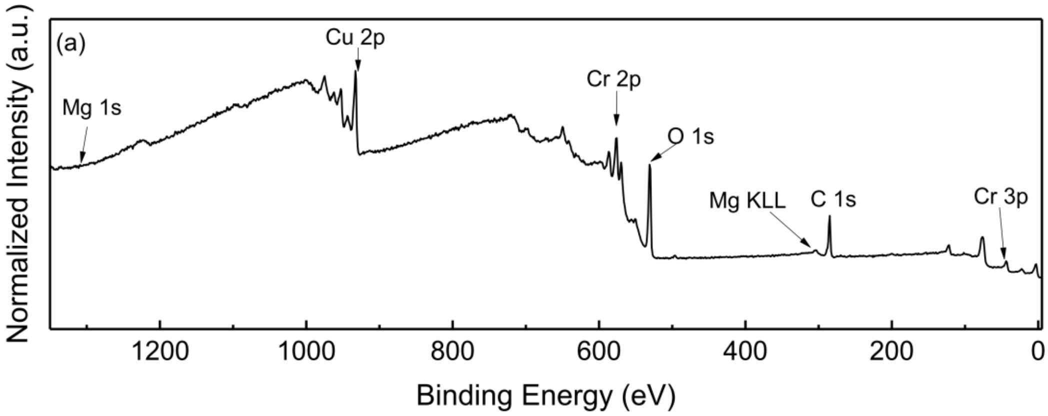

Figure S6. XPS spectra and respective fittings of Cu 2p, Cr 2p and O 1s regions for a typical Mg-doped $CuCrO_2$ sample.

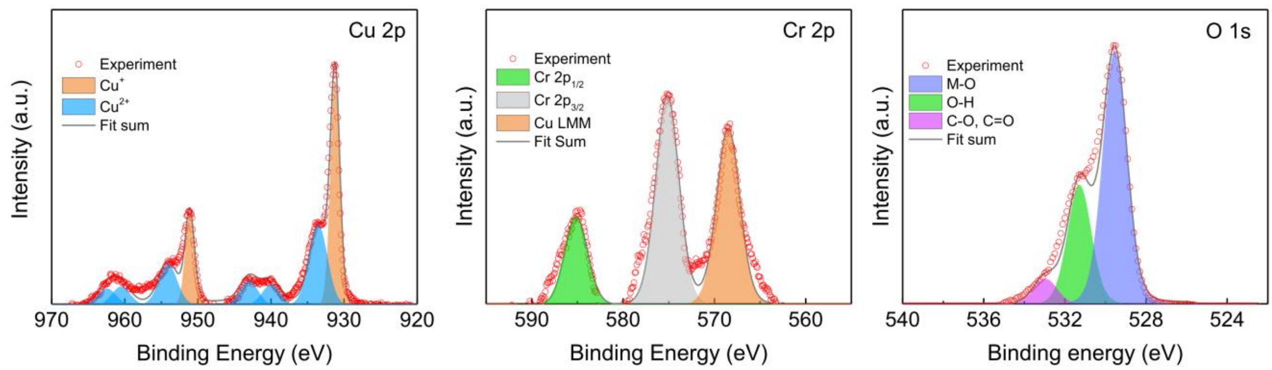

Figure S7. XPS spectra of a) Cr 3p and Mg 2p region, and b) valence band (VB) region at various Mg concentrations.

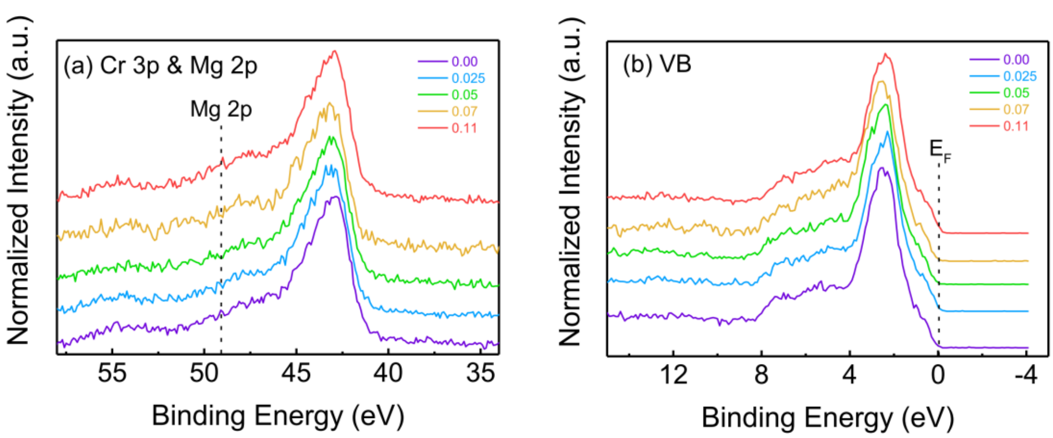

Figure S8. Average visible transmittance (wavelength between 400 nm to 800 nm) for $CuCrO_2$ films as a function of Mg concentration. The black triangle shows the value for a conventional, copper-rich film.

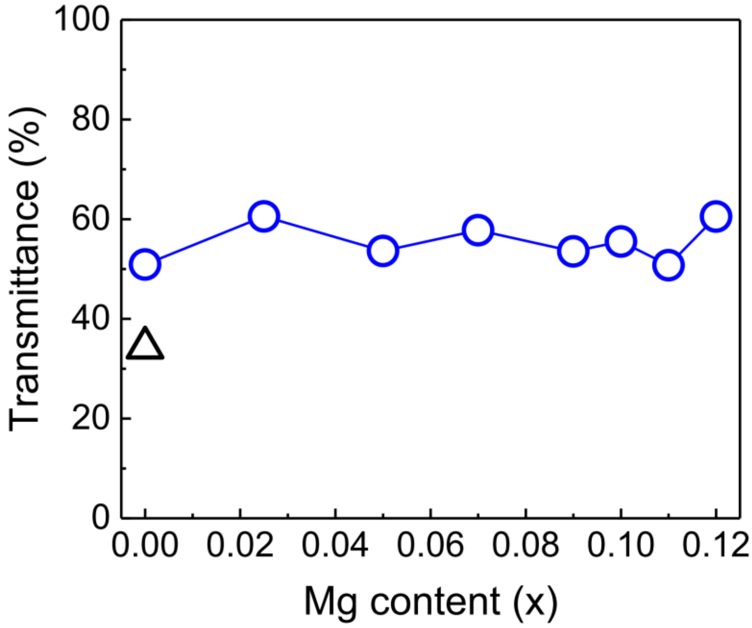

Figure S9. Absorptance (A) spectra for undoped $CuCrO_2$ films on borosilicate glass prepared from copper-deficient precursors (nominally $[Cu_{0.4}Cr_{0.6}O]_2$) and stoichiometric precursors (nominally $[Cu_{0.5}Cr_{0.5}O]_2$). These have been calculated from Transmittance (T) and reflectance (R) spectra, through the relationship A = 100 – T – R (%).

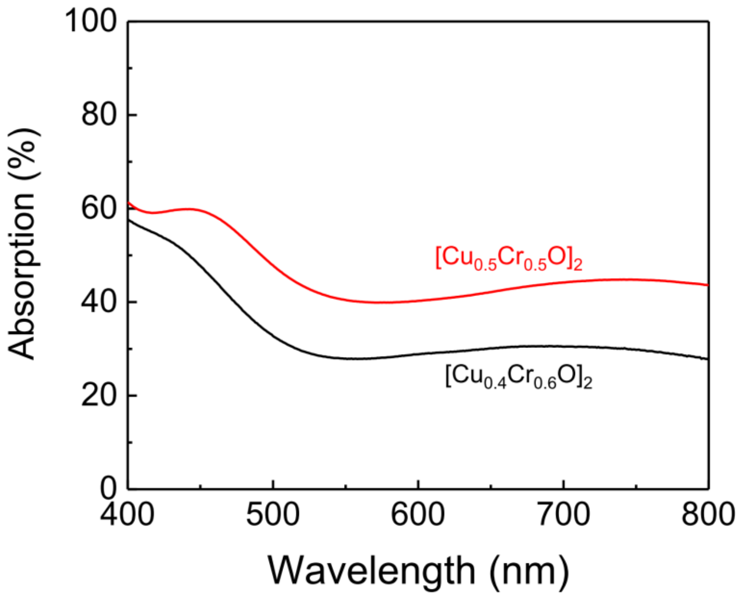

Figure S10. Reflectance spectra for $CuCrO_2$ films as a function of the Mg dopant concentration. The inset shows the average reflectance in the visible region (400 nm to 800 nm).

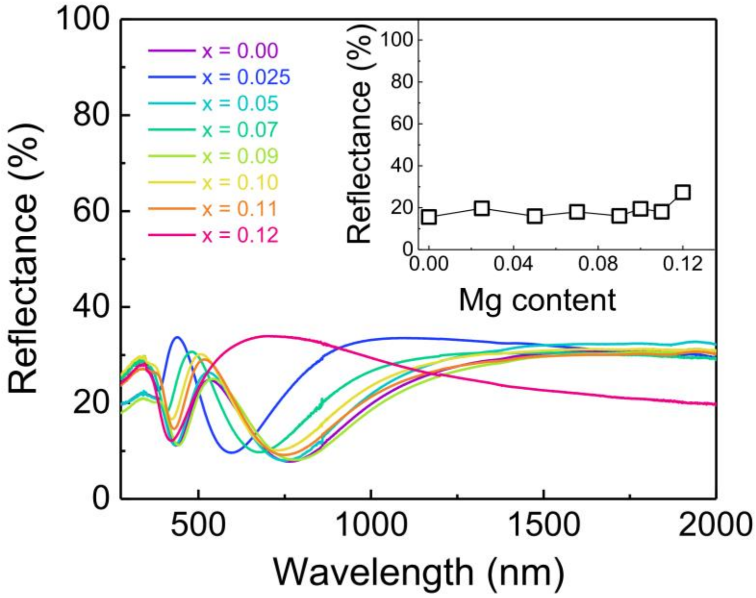

Table S1. Compositional analysis obtained via EDX. The incorporation efficiency quantifies the amount (in %) of Mg that was detected in the films, compared to the amount of Mg used in the precursor solution.

Nominal Mg (%)	Real Mg (%)	Incorporation efficiency (%)	Nominal Cu (%)	Nominal (Cr+Mg) (%)	Real Cu (%)	Real (Cr+Mg) (%)
0	0.12±0.31	N/A	40	60	49.3±0.6	50.7±1.7
2.5	0.68±0.32	27.2	40	60	50.4±1.4	49.6±2.2
5	1.14±0.28	22.8	40	60	49.9±1.0	50.1±2.9
7	1.90±0.30	27.1	40	60	51.7±1.1	48.3±3.4
11	3.02±0.25	27.4	40	60	50.2±0.8	49.8±2.0

Table S2. Values for visible transmittance vs. conductivity for $CuCrO_2$ and $CuGaO_2$ films reported in the literature and for some of the best samples presented in this study.

Material	Conductivity ($S\ cm^{-1}$)	Vis. transmittance (%)	Reference
$CuCrO_2$	0.017	60	[1]
$CuCrO_2$	0.140	70	[2]
$CuCrO_2$	50	52	[3]
$CuCrO_2$	0.232	62	[4]
$CuCrO_2$	35	51	[5]
$CuCrO_2$	0.083	55	[6]
$CuCrO_2$	0.25	55	[7]
$CuCrO_2$	17	40	[8]
Mg-doped $CuCrO_2$	0.136	65	[9]
Mg-doped $CuCrO_2$	1.0	80	[10]
Mg-doped $CuCrO_2$	2.174	57	[11]
Mg-doped $CuCrO_2$	220	30	[12]
Mg-doped $CuCrO_2$	217	70	[13]
Zn-doped $CuCrO_2$	0.262	68	[14]
$CuGaO_2$	0.063	80	[15]
$CuGaO_2$	0.015	80	[16]
$CuGaO_2$	0.004	60	[17]
This work[a]			
$[Cu_{0.4}Cr_{0.575}Mg_{0.025}O]_2$	13.3	60.5	This work
$[Cu_{0.4}Cr_{0.55}Mg_{0.05}O]_2$	21.2	53.6	This work
$[Cu_{0.4}Cr_{0.53}Mg_{0.07}O]_2$	19.2	57.8	This work
$[Cu_{0.4}Cr_{0.50}Mg_{0.10}O]_2$	26.8	55.5	This work
$[Cu_{0.4}Cr_{0.49}Mg_{0.11}O]_2$	52.8	50.8	This work
$[Cu_{0.4}Cr_{0.48}Mg_{0.12}O]_2$	44.5	60.5	This work

[a] the compositions listed are nominal, based on the amount of precursors used

References

1. Han, M., et al., *Structural, electronic band transition and optoelectronic properties of delafossite CuGa1xCrxO2 (0 x 1) solid solution films grown by the sol-gel method.* 2012. **22**(35): p. 18463-1847.
2. Wang, J., et al., *Combustion Synthesis of p-Type Transparent Conducting CuCrO2+x and Cu:CrOx Thin Films at 180 °C.* ACS Applied Materials & Interfaces, 2018. **10**(4): p. 3732-3738.
3. Bottiglieri, L., et al., *Out of stoichiometry CuCrO 2 films as a promising p-type TCO for transparent electronics.* Materials advances, 2021. **2**(14): p. 4721-4732.
4. Yu, R.-S. and C.-M. Wu, *Characteristics of p-type transparent conductive CuCrO2 thin films.* Applied surface science, 2013. **282**: p. 92-97.
5. Sánchez-Alarcón, R.I., et al., *Ultrasonic spray-pyrolyzed CuCrO2 thin films.* Journal of physics. D, Applied physics, 2016. **49**(17).
6. Farrell, L., et al., *Spray pyrolysis growth of a high figure of merit, nano-crystalline, p -type transparent conducting material at low temperature.* Applied physics letters, 2015. **107**(3).
7. Farrell, L., et al., *Synthesis of nanocrystalline Cu deficient CuCrO2 - a high figure of merit p-type transparent semiconductor.* Journal of materials chemistry. C, Materials for optical and electronic devices, 2016. **4**(1): p. 126-134.
8. Crêpellière, J., et al., *Transparent conductive CuCrO2 thin films deposited by pulsed injection metal organic chemical vapor deposition: up-scalable process technology for an improved transparency/conductivity trade-off.* 2016. **4**(19): p. 4278-4287.
9. Wang, Y., et al., *Structural, optical and electrical properties of Mg-doped CuCrO2 thin films by sol—gel processing.* Journal of alloys and compounds, 2011. **509**(19): p. 5897-5902.

10. Lim, S.H., S. Desu, and A.C. Rastogi, *Chemical spray pyrolysis deposition and characterization of p-type CuCr1-xmgxO2 transparent oxide semiconductor thin films.* The Journal of physics and chemistry of solids, 2008. **69**(8): p. 2047-2056.

11. Ohno, K., et al., *Effect of forming gas annealing on improvement in crystal orientation of solid-phase calcined CuCrO2 thin film.* Thin solid films, 2020. **714**: p. 138386.

12. Nagarajan, R., et al., *p-type conductivity in CuCr1−xMgxO2 films and powders.* Journal of Applied Physics, 2001. **89**(12): p. 8022-8025.

13. Tripathi, T.S. and M. Karppinen, *Enhanced p-Type Transparent Semiconducting Characteristics for ALD-Grown Mg-Substituted CuCrO2 Thin Films.* Advanced electronic materials, 2017. **3**(6): p. n/a.

14. Yu, R.-S. and C. Chu, *Synthesis and Characteristics of Zn-Doped CuCrO2 Transparent Conductive Thin Films.* Coatings (Basel), 2019. **9**(5): p. 321.

15. Ueda, K., et al., *Epitaxial growth of transparent p-type conducting CuGaO 2 thin films on sapphire (001) substrates by pulsed laser deposition.* Journal of Applied Physics, 2001. **89**(3): p. 1790-1793.

16. Alias, A., et al., *Characterization of CuGaO2 films prepared by sol-gel methods.* physica status solidi c, 2012. **9**(2): p. 198-201.

17. Ehara, T., *Preparation of CuGaO2 thin film by a sol-gel method using two kinds of metal source combination.* Journal of Materials Science and Chemical Engineering, 2018. **6**(8): p. 68-78.